Supplemental Information

Biochemical, Biophysical, and Immunological Characterization of Respiratory Secretions in Severe SARS-CoV-2 (COVID-19) Infections

Michael J. Kratochvil[1,2#], Gernot Kaber[1#], Sally Demirdjian[1#], Pamela C. Cai[3], Elizabeth B. Burgener[4], Nadine Nagy[1], Graham L. Barlow[1], Medeea Popescu[1], Mark R. Nicolls[5], Michael G. Ozawa[6], Donald P. Regula[6], Ana E. Pacheco-Navarro[5], Samuel Yang[7], Vinicio A. de Jesus Perez[5], Harry Karmouty-Quintana[8,9], Andrew M. Peters[8], Bihong Zhao[10], Maximilian L. Buja[10], Pamela Y. Johnson[11], Robert B. Vernon[11], Thomas N. Wight[11], Stanford COVID-19 Biobank Study Group, Carlos E. Milla[4*], Angela J. Rogers[5*], Andrew J. Spakowitz[3*], Sarah C. Heilshorn[2*] and Paul L. Bollyky[1*]

Table of Contents

Supplemental Table 1. Demographic details of healthy cohort

Characteristic	Adult cohort *(n=6)*
Age (years)	42.8 (31 - 58)
Male gender	5 (83.3%)
Race/Ethnicity	Non-black Hispanic 1 (16.7%) White 5 (83.3%)
Preexisting diabetes mellitus	0 (0%)
Preexisting pulmonary disease	0 (0%)
Preexisting cardiac disease	0 (0%)

Supplemental Table 2. Histologic staining results of lung tissues for HA, versican, and TSG6.

Patient identifier	Stain	Group	Histopathology results
1012A	HABP-B	Healthy	Mild staining of the alveolar-capillary membrane. Strong adentitia and peribronchial staining.
1012A	Versican	Healthy	Strong bronchial epithelial staining, mild to moderate perbronchial staining, mild perivascular stain
1012A	TSG6	Healthy	Strong staining of bronchial epithelium and alveolar macrophages. Some alveolar epithelial cells also show mild staining.
1051D	HABP-B	Healthy	Moderate staining in the bronchial wall, vascular adventitia and alveolar-capillary membrane. Alveolar macrophages also exhibit strong intracellular staining.
1051D	Versican	Healthy	Strong adventitial stain around medium around small pulmonary arteries. No bronchial epithelium stainin. Medium to strong peribronchial staining.
1051D	TSG6	Healthy	Strong staining of bronchial epithelium and alveolar macrophages. Mild to medium stain of medial layer of pulmonary arteries. Strong alveolar epithelial staining.
1007A	HABP-B	Healthy	Strong staining in the bronchial wall, vascular adventitia and alveolar-capillary membrane. Mild to mderate staining in the basement membrane of medium size vessels.
1007A	Versican	Healthy	Strong alveolar macrophage staining. Mild stain of pulmonary veins. Strong bronchial epithelial and peribronchial staining. Strong staining in basement membrane and adventitia of pulmonary arteries.
1007A	TSG6	Healthy	Strong bronchial epithelial stain, Strong alveolar macrophage stain,mild to moderate alveolar-capillary stain, no stain of the small pulmonary vessels (50um); mild subendothelial staining of medium size vessels.
1041D	HABP-B	Healthy	Strong staining in the bronchial wall, veins, vascular adventitia and alveolarcapillary membrane. Mild to mderate staining in the basement membrane of medium size vessels.
1041D	Versican	Healthy	Strong alveolar macrophage staining. Mild stain of pulmonary veins. Strong bronchial epithelial and peribronchial staining. Strong staining in basement membrane and adventitia of pulmonary arteries.

1041D	TSG6	Healthy	Strong staining of bronchial epithelium and alveolar macrophages. Some alveolar epithelial cells also show mild staining.
87H	HABP-B	Healthy	Relative well preserved lung tissue with minimal peribronchial inflammation. Staining can be seen in parenchyma with stronger staining in airway and vascular media.
87H	Versican	Healthy	Faint stain throughout, stronger in internal and external elastic lamina of blood vessels.
87H	TSG6	Healthy	Faint stain, relatively well preserved parenchyma, some staining in the intimal layer of blood vessels, strong stain in perivascular inflammatory cells
HA20-44	HABP-B	COVID-19 ARDS	Lung shows evidence of extensive consolidation with epithelial detachment and hemorrhage. Strong diffuse staining in areas of necrosis and inflammation. Strong staining across the entire wall of medium sized vessels.
HA20-44	Versican	COVID-19 ARDS	Strong stain adjacent to the external elastic lamina of small and medium size arteries and veins, strong stain in the basement membrane of alveolar epithelial cells.
HA20-44	TSG6	COVID-19 ARDS	Mild to moderate staining of the alveolar macrophages and other immune cells infiltrating the parenchyma. Moderate to strong staining of alveolar epithelium and endothelial layer of vessels.
HA20-36	HABP-B	COVID-19 ARDS	Lung shows complete consolidation with epithelial detachment, hemorrhage, and necrosis. No intact alveolar structure can be appreciated. Strong staining across the entire wall of medium sized vessels.
HA20-36	Versican	COVID-19 ARDS	Strong stain adjacent to the external elastic lamina of small and medium size arteries and veins, Large vessels show strong staining across the entire wall.
HA20-36	TSG6	COVID-19 ARDS	Moderate to strong staining of immune cells infiltrating the parenchyma. Moderate to strong staining of endothelial layer of vessels.
HA20-39	HABP-B	COVID-19 ARDS	Diffuse alveolar hemorrhage, distended alveolar-capillary membrane with strong heterogeneous staining; diffuse bronchial and vascular staining.
HA20-39	Versican	COVID-19 ARDS	Strong stain within medial layer of large to small size arteries, moderate to strong staining in the alveolar-capillary membrane.

HA20-39	TSG6	COVID-19 ARDS	Moderate staining of immune cells infiltrating the parenchyma. Mild staining of medial layer of vessels. Staining in alveolar-capillary membrane likely represents immune cells.
HA20-55	HABP-B	COVID-19 ARDS	Diffuse alveolar hemorrhage, distended alveolar-capillary membrane with strong heterogeneous staining; diffuse bronchial and vascular staining.
HA20-55	Versican	COVID-19 ARDS	Strong stain within medial layer of large to small size arteries, mild staining in the alveolar-capillary membrane. One large vessels with diffuse strong staining can be seen at the center of the slide.
HA20-55	TSG6	COVID-19 ARDS	Mild stain of the alveolar macrophages and other immune cells.
603	HABP-B	COVID-19 ARDS	Diffuse alveolar hemorrhage, distended alveolar-capillary membrane with strong heterogeneous staining; diffuse bronchial and vascular staining.
603	Versican	COVID-19 ARDS	Strong stain within the subendothelial and adventitial layer of large to small size arteries, moderate to strong staining in the alveolar-capillary membrane.
603	TSG6	COVID-19 ARDS	Mild stain of the alveolar macrophages and other immune cells. Heterogeneous stain of intima and adventita of medium sized vessels.
HA20-16	HABP-B	non-COVID-19 ARDS	Strong signal in medium pulmonary arteries, particularly in the adventitial layer, and immune cells. Mild to moderate stain in the alveolar-capillary membrane
HA20-16	Versican	non-COVID-19 ARDS	Strong stain within medial layer of large to small size arteries, moderate staining in the alveolar-capillary membrane.
HA20-16	TSG6	non-COVID-19 ARDS	Mild staining of alveolar macrophages and other immune cells.
HA19-113	HABP-B	non-COVID-19 ARDS	Diffuse stain across the lung tissue. No discernible structures in most of the sample due to massive cell immune infiltration and tissue destruction.
HA19-113	Versican	non-COVID-19 ARDS	Strong stain within medial layer of large to small size arteries, mild staining in the alveolar-capillary membrane.
HA19-113	TSG6	non-COVID-19 ARDS	Mild staining of alveolar macrophages and other immune cells, Scattered staining of endothelial cells in medium size vessels.

HA20-30	HABP-B	non-COVID-19 ARDS	Strong signal intensity in the alveolar-capillary membrane. Alveolar macrophages and other immune cells within alveoli have mild or no stain.
HA20-30	Versican	non-COVID-19 ARDS	Strong stain within medial layer of large to small size arteries, mild to moderate staining in the alveolar-capillary membrane.
HA20-30	TSG6	non-COVID-19 ARDS	Strong staining of alveolar macrophages and other immune cells. Strong staining of alveolar epithelium.
HA20-98	HABP-B	non-COVID-19 ARDS	Strong signal intensity in the alveolar-capillary membrane. Strong perivascular staining.
HA20-98	Versican	non-COVID-19 ARDS	Strong stain within medial layer of large to small size arteries, moderate to high staining in the alveolar-capillary membrane.
HA20-98	TSG6	non-COVID-19 ARDS	Mild staining of alveolar macrophages and other immune cells.
51L	HABP-B	CF	Diffuse stain -stronger around medial layer of blood vessels and airways
51L	Versican	CF	Strong stain of the medial layer of medium and small muscularized vessels. Staining can also be seen inside alveolar type 1 and 2 epithelial cells
51L	TSG6	CF	Faint staining throughout; strong stain in subendothelial layer, strongest in inflammatory cells within alveoli.
38A	HABP-B	CF	Diffuse stain -stronger around medial layer of blood vessels and airways; several inflammatory clusters.
38A	Versican	CF	Strong stain of the medial layer of medium and small muscularized vessels; strong stain in bronchial submucosa.
38A	TSG6	CF	Strong stain on mucus and bronchial epithelial cells.
46 O	HABP-B	CF	Diffuse stain -stronger around medial layer of blood vessels and airways, mucus pools seen in alveoli and bronchial lumen also stain positive.
46 O	Versican	CF	Diffuse parenchymal staining, strong stain in bronchial mucosa around engorged glands.
46 O	TSG6	CF	Strong stain in bronchial epithelium, inflammatory cells, medium stain in vascular media.
S08 33829 F	TSG6	Lung tumor	Staining controls
S08 33829 F	Rbt IgG	Lung tumor	Staining controls

QC 0100 A2	TSG6	Kidney (Pan QC0020A3)	Staining controls
S10-03891	Versican	Human lung tumor	Staining controls
S10-03891	Rbt IgG	Human lung tumor	Staining controls
A 14-20-16	Versican	DIVA CF lung	Staining controls
A 14-20-16	Rbt IgG	DIVA CF lung	Staining controls

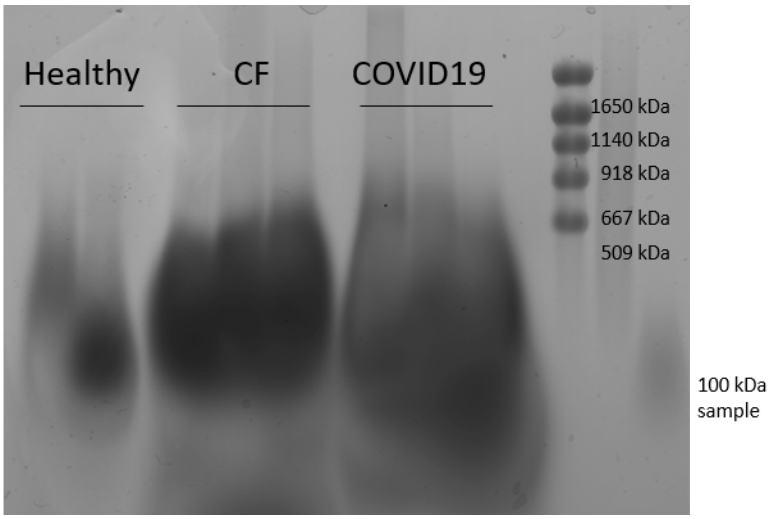

Supplemental Figure 1. Representative HA molecular weight sizing gel from Healthy, CF, and COVID-19 respiratory secretion samples.

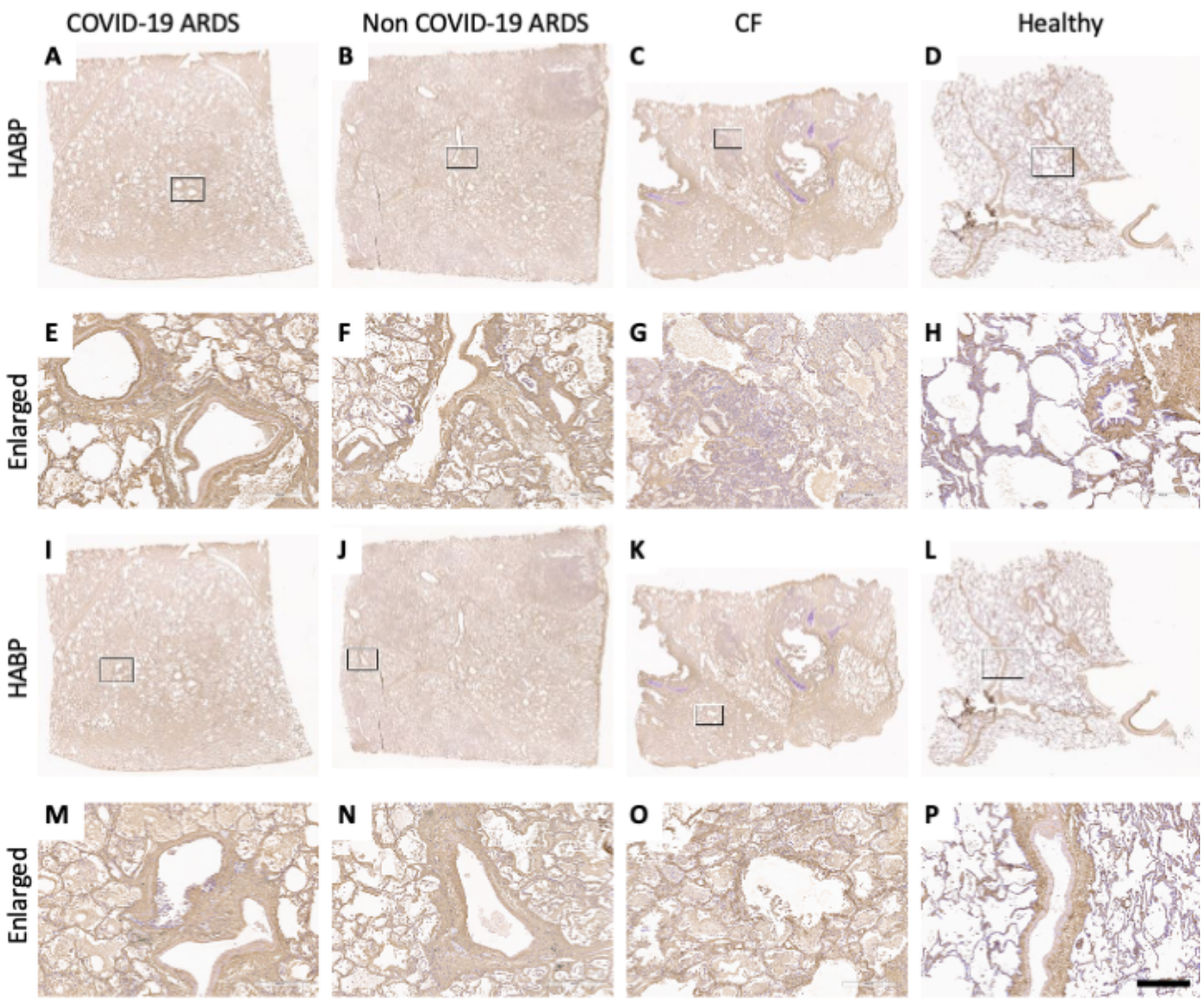

Supplemental Figure 3. HA accumulation and distribution in COVID-19 ARDS, non-COVID ARDS, CF and healthy lung sections. Representative histological cadaveric lung sections from donors with COVID-19 ARDS, donors with non-COVID-19 ARDS, donors with CF, and healthy donors stained with (**A-P**) HABP. (**E-H**) and (**M-P**) are enlarged sections from (**A-D**) and (**I-L**) respectively (box highlights enlarged area). Nuclei are stained in blue, and HABP is stained in brown. Scale bar A-P 400 μm. Whole-section imaging was performed using a Aperio (Leica) AT2 Digital Pathology whole slide scanner. Slides were scanned in bright-field at a 20× objective and the digital images imported for analysis using the Aperio Imagescope v12.4.3.5008 viewing software.

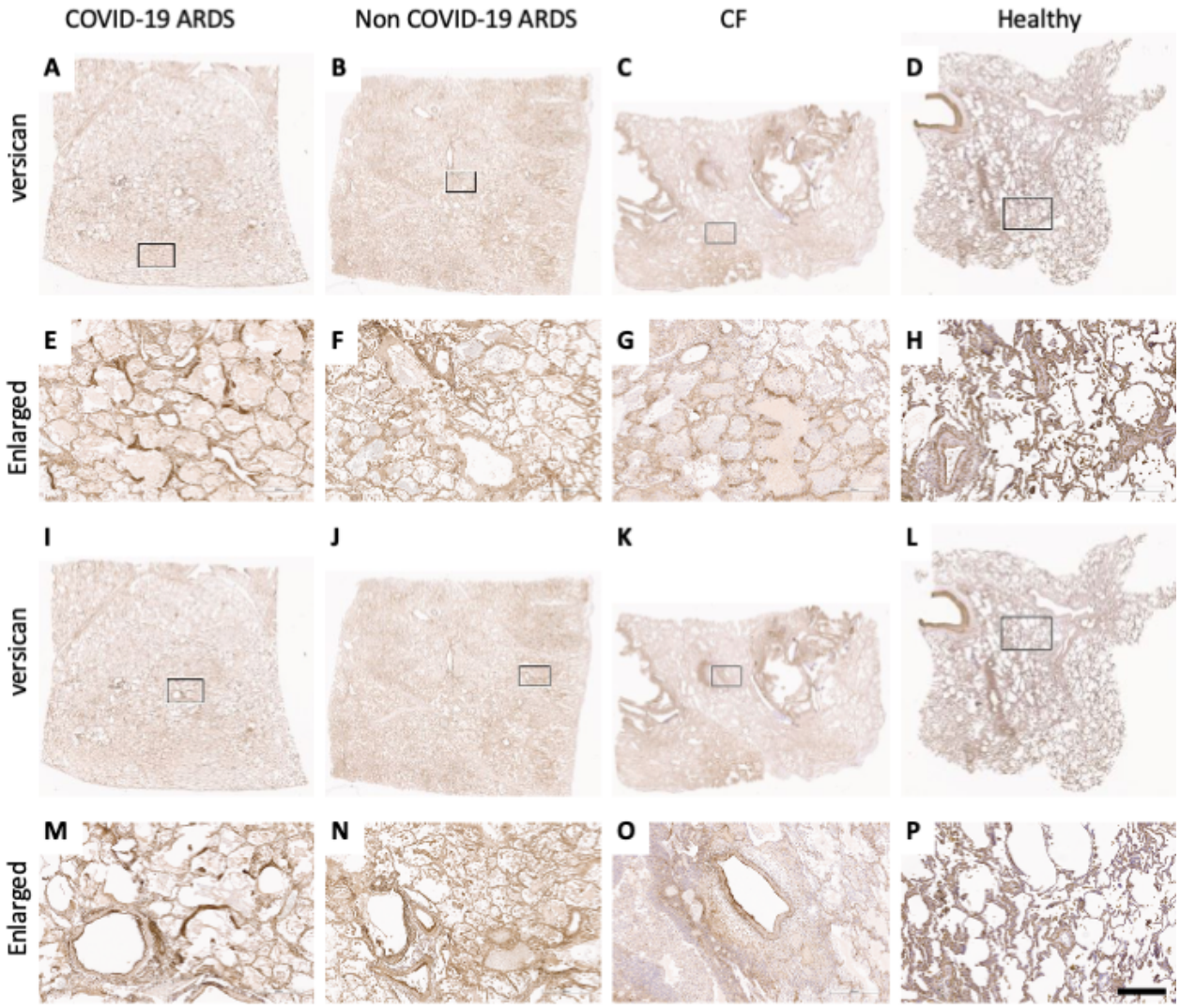

Supplemental Figure 4. Versican accumulation and distribution in COVID-19 ARDS, non-COVID ARDS, CF and healthy lung sections. Representative histological cadaveric lung sections from donors with COVID-19 ARDS, donors with non-COVID-19 ARDS, donors with CF, and healthy donors stained with (**A-P**) Versican. (**E-H**) and (**M-P**) are enlarged sections from (**A-D**) and (**I-L**) respectively (box highlights enlarged area). Nuclei are stained in blue, and HABP is stained in brown. Scale bar A-P 400 μm. Whole-section imaging was performed using a Aperio (Leica) AT2 Digital Pathology whole slide scanner. Slides were scanned in bright-field at a 20× objective and the digital images imported for analysis using the Aperio Imagescope v12.4.3.5008 viewing software.

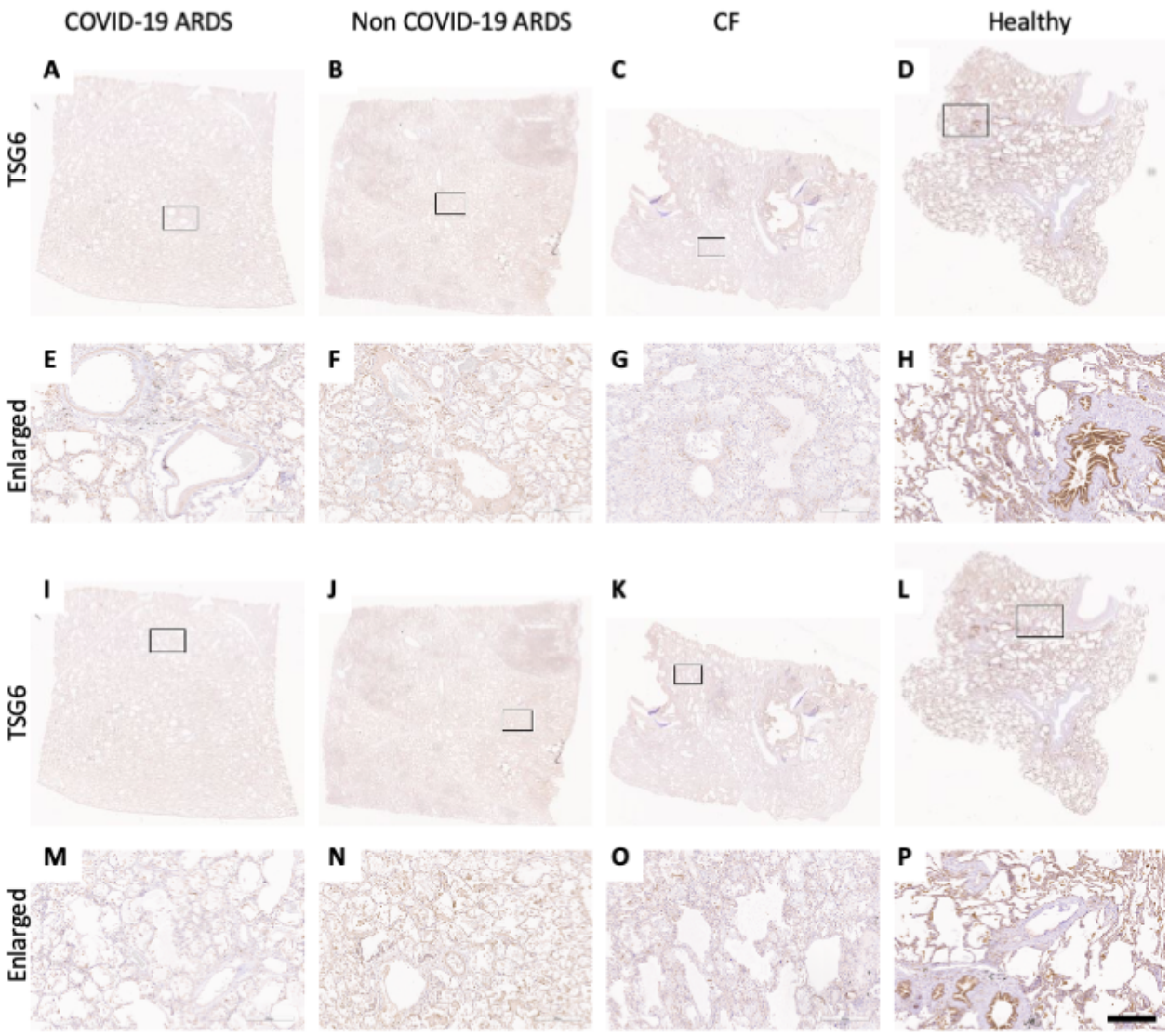

Supplemental Figure 5. TSG6 accumulation and distribution in COVID-19 ARDS, non-COVID ARDS, CF and healthy lung sections. Representative histological cadaveric lung sections from donors with COVID-19 ARDS, donors with non-COVID-19 ARDS, donors with CF, and healthy donors stained with (**A-P**) TSG6. (**E-H**) and (**M-P**) are enlarged sections from (**A-D**) and (**I-L**) respectively (box highlights enlarged area). Nuclei are stained in blue, and HABP is stained in brown. Scale bar A-P 400 μm. Whole-section imaging was performed using a Aperio (Leica) AT2 Digital Pathology whole slide scanner. Slides were scanned in bright-field at a 20× objective and the digital images imported for analysis using the Aperio Imagescope v12.4.3.5008 viewing software.

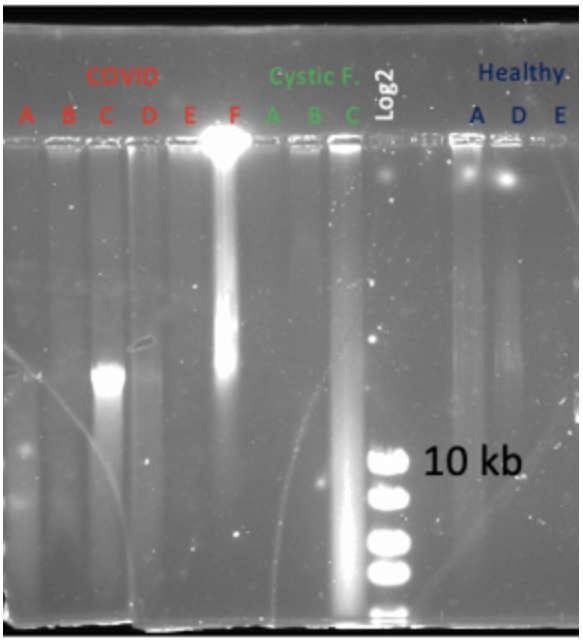

Supplemental Figure 5. Representative DNA molecular weight sizing gel from Healthy, CF, and COVID-19 respiratory secretion samples.

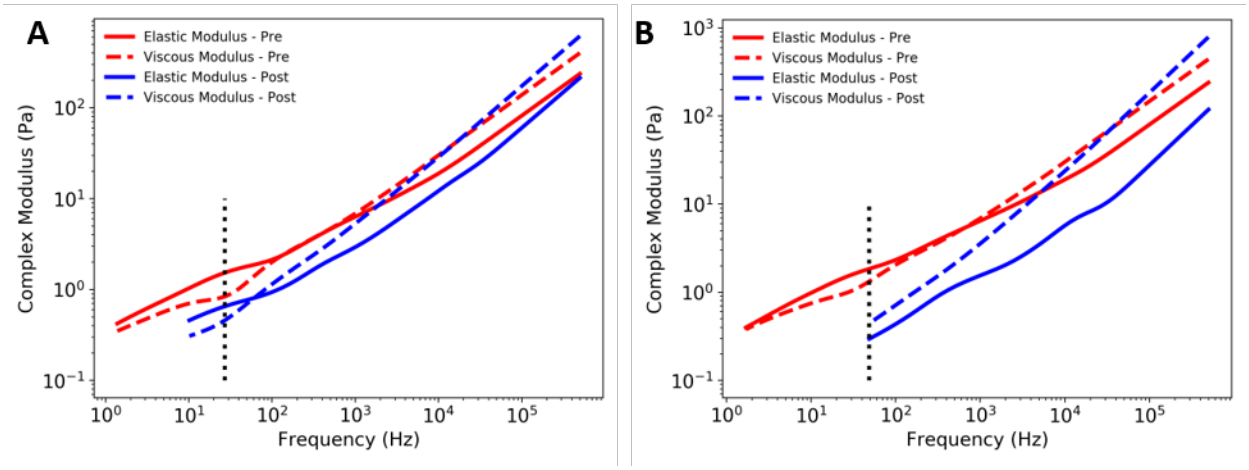

Supplemental Figure 6. Representative rheological spectra for pre-treatment and post-treatment samples, where the dotted line represents the frequency chosen at which the single modulus value was used for comparison when (**A**) a "plateau" region of the elastic modulus exists or, (**B**) in the case of no plateau region and hence the lowest frequency is selected.

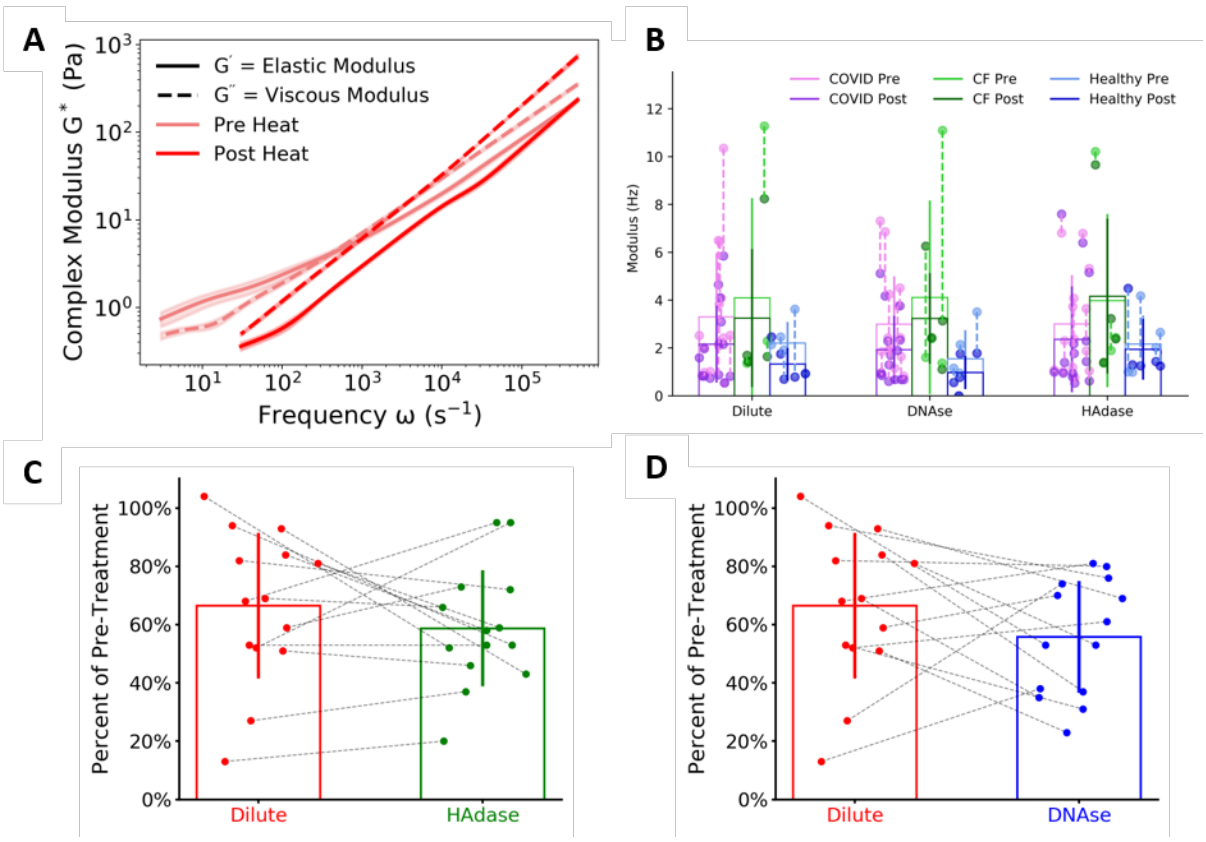

Supplemental Figure 7. (**A**) Microrheology data showing the impact of virus-killing heat treatment on cystic fibrosis (CF) respiratory secretions. (**B**) A plot of the measured moduli of all samples tested. Lighter and darker data points indicate the pre- and post-treatment, respectively, with a dashed line connecting data from the same patient sample. (**C**) A plot of relative change in modulus of COVID-19 respiratory secretions after dilution or HAdase enzymatic treatment compared to pre-treatment modulus, with a dashed line connecting data points generated from the same patient sample (n=14). (**D**) A plot of relative change in modulus of COVID-19 respiratory secretions after dilution or DNase enzymatic treatment compared to pre-treatment modulus, with a dashed line connecting data points generated from the same patient sample (n=14).

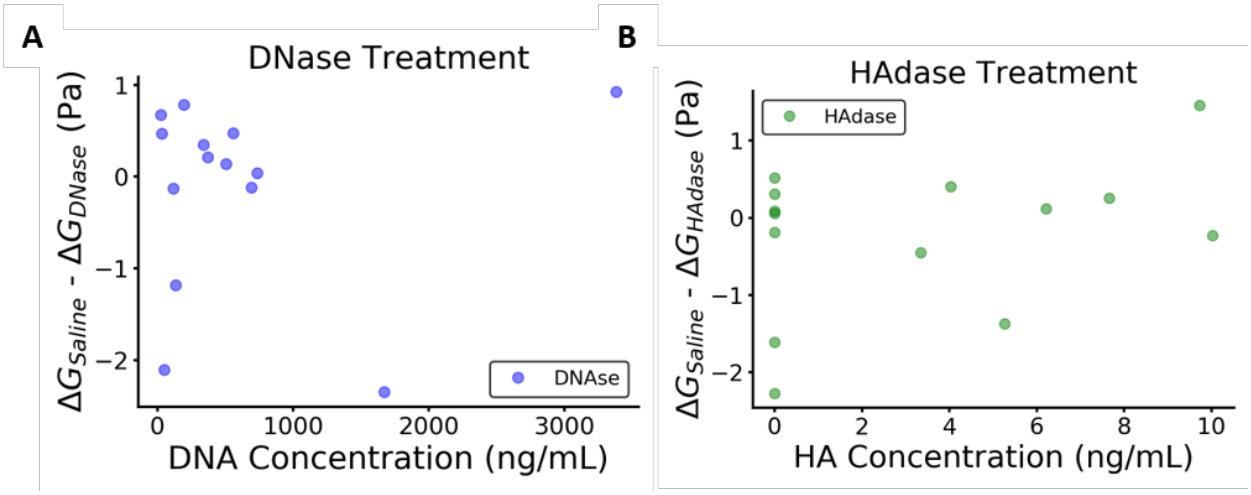

Supplemental Figure 8. Impact of concentration of DNA and HA on the modulus change due to enzymatic treatment**.** (**A**) The difference in modulus of COVID-19 lung secretions upon control saline dilution and enzymatic DNAase treatment (ΔG_{Saline}-ΔG_{DNase}) versus the initial, pre-treatment modulus (blue) (n=14). (**B**) The difference in modulus of COVID-19 lung secretions upon control saline dilution and enzymatic HAdase treatment (ΔG_{Saline}-ΔG_{HAdase}) versus the initial, pre-treatment modulus (green) (n=14). We found no strong correlation between biopolymer concentration and modulus change as indicated by the Bayesian Information Criterion (BIC) values being less than 10 (3.5 and 8.5 for DNA and HA).

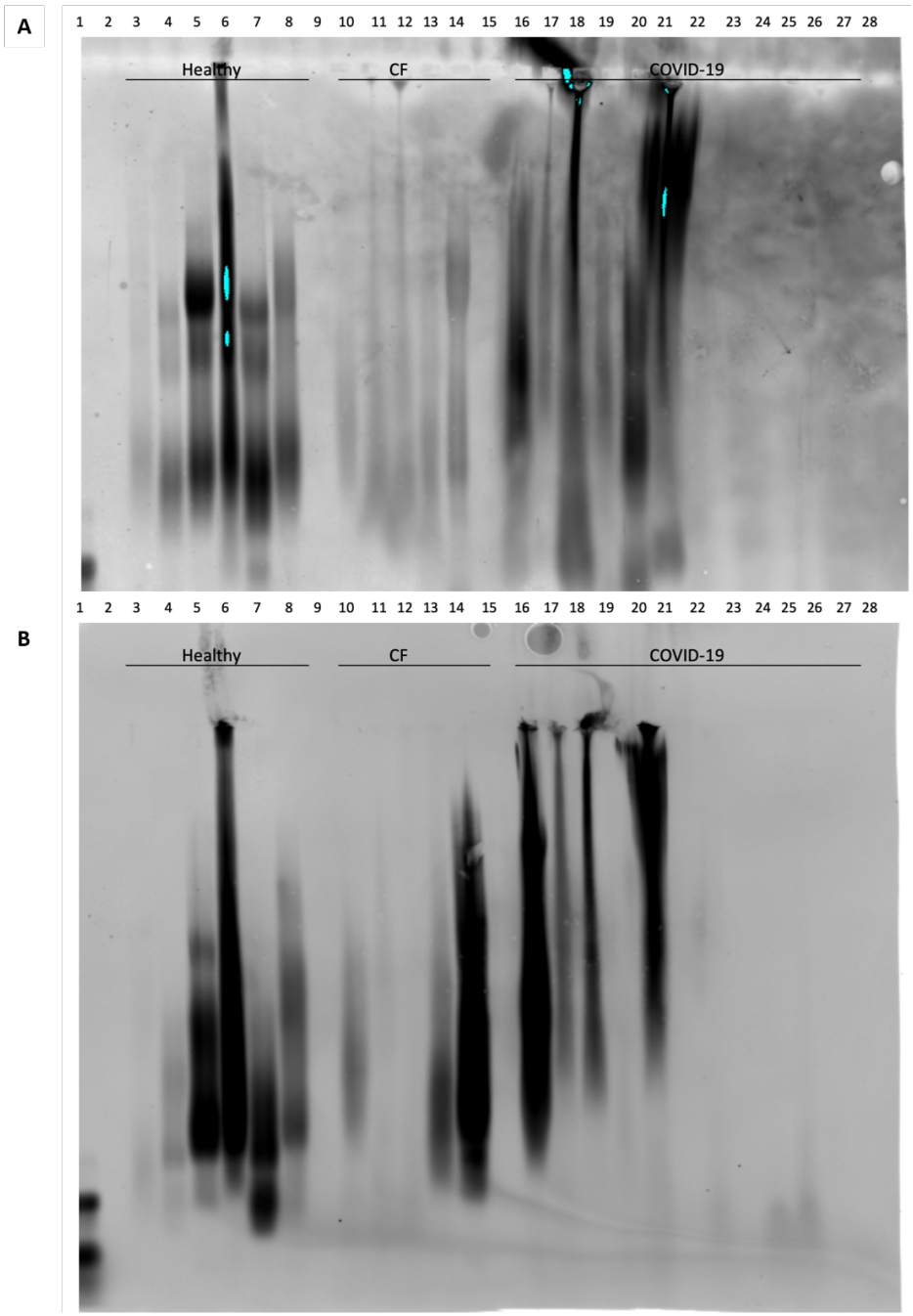

Supplemental Figure 9. Representative western blot analysis of MUC5AC and MUC5B protein expression from Healthy (n-6), CF (n=5), and COVID-19 respiratory secretion samples (n=12 for A, n=11 for B). Samples were separated via mucin agarose Western blotting and the membrane was probed with a (**A**) rabbit MUC5AC polyclonal antibody (**B**) mouse MUC5B (A-3) monoclonal antibody. In panel A, lanes 2, 9, 15, 22, 28 are blank, while in panel B lanes 2, 9, 15, 21, 28 are blank.

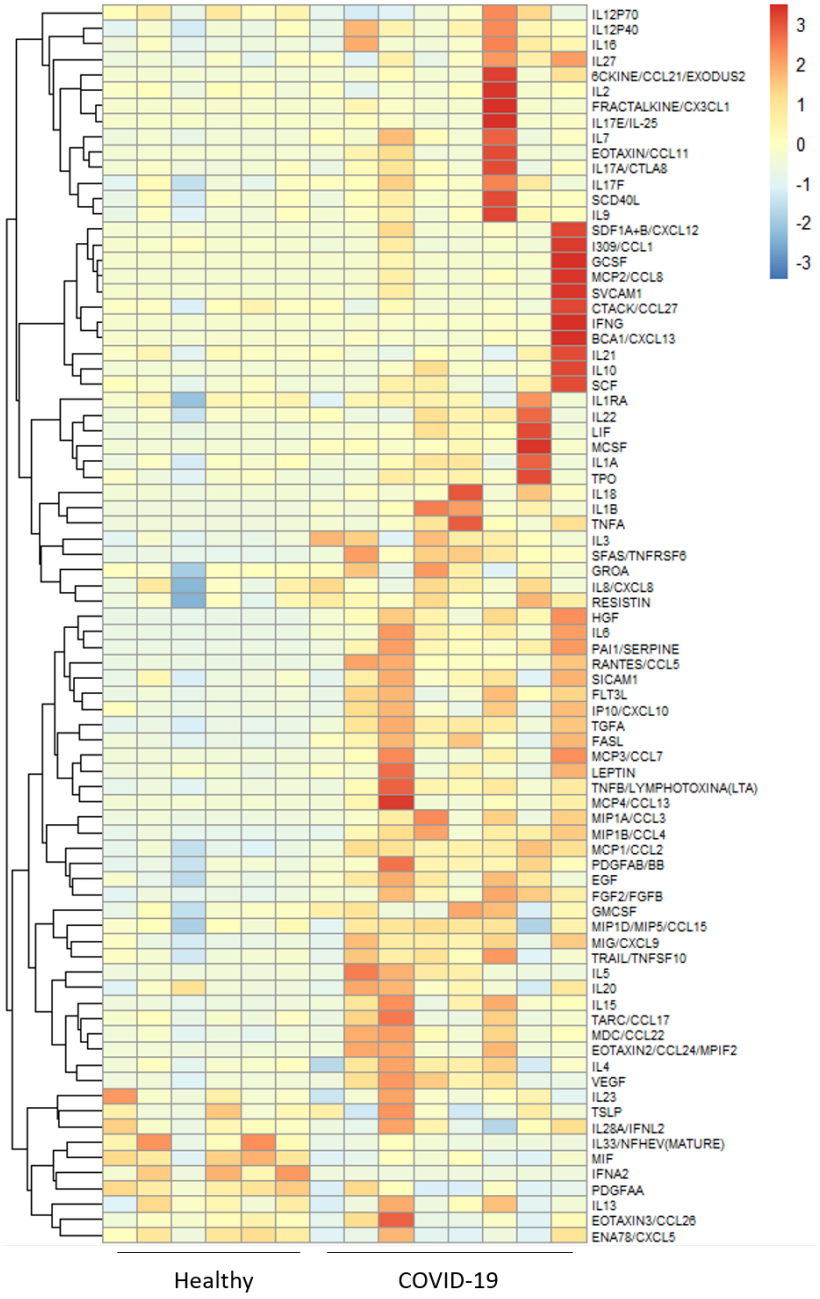

Supplemental Figure 10. Heat map of raw mean fluorescence intensity (MFI) data scaled per row (Healthy vs COVID-19). Cytokines, chemokines, adhesion molecules, and growth factors were measured in the respiratory secretion samples of healthy controls (n = 6) and in COVID-19 ARDS patients (n=8) using a bead-based multiplexed immunoassay system, Luminex-EMD Millipore Human 80 Plex assays. Upregulated cytokines are shown in orange and downregulated in blue.

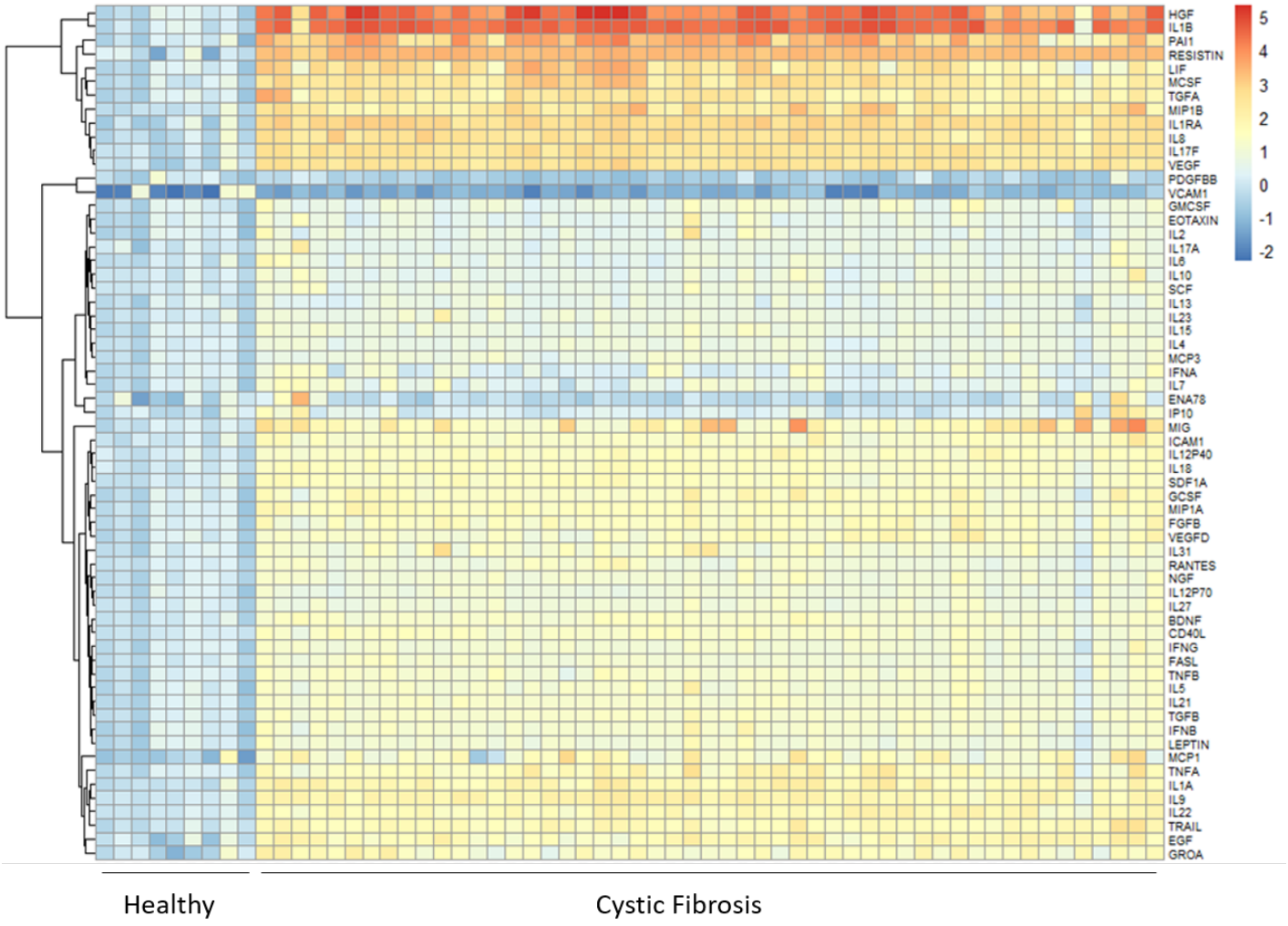

Supplemental Figure 11. Immunological characterization of respiratory secretions from CF patients. Heat map of mean fluorescence intensity (MFI) data, log2 transformed, and normalized to average of the healthy controls per cytokine. Data are ordered by KNN clustering of the cytokines (y-axis). Cytokines, chemokines, adhesion molecules, and growth factors were measured in the respiratory secretion samples of healthy controls (n = 9) and in adult CF patients (n=51) using a bead-based multiplexed immunoassay system, Luminex-EMD Millipore Human 63 Plex assays. Upregulated cytokines are shown in orange and downregulated in blue.

Supplemental Methods

Western blot analysis to characterize mucins: Respiratory secretion samples, normalized by weight, were mixed with loading solution, and subjected to Western blot analysis as previously described (doi:10.3791/54153). Briefly, the samples were separated on a 1% agarose gel in 1X TAE-0.1% SDS at 80 V, transferred to nitrocellulose membranes and blocked in 2% Casein, 1% BSA solution. Mucin 5B (MUC5B) was detected with the mouse MUC5B (A-3) monoclonal antibody (sc-393952, Santa Cruz Biotechnology) at 1ug/ml, followed by donkey anti-mouse AF800 secondary antibody (1:10,000). Mucin 5AC (MUC5AC) was detected with the rabbit MUC5AC polyclonal antibody (Thermofisher Scientific) at 0.5ug/ml, followed by goat anti-rabbit AF800 secondary antibody (1:10,000). The blots were imaged on a LI-COR Odyssey Western Blot Imaging system.

Supplemental Acknowledgements

The Stanford COVID-19 Biobank Study Group is: Rosen Mann, Anita Visweswaran, Thanmayi

Ranganath, Jonasel Roque, Monali Manohar, Hena Naz Din, Komal Kumar, Kathryn Jee, Brigit

Noon, Jill Anderson, Bethany Fay, Donald Schreiber, Nancy Zhao, Rosemary Vergara,

Catherine Blish, Kari Nadeau, Andra Blomkalns, Ruth O'Hara. The affiliation for all members is: Stanford University School of Medicine, Stanford, California, USA.